Hybrid PV and Battery System Sizing for Commercial Buildings in Malaysia: A Case Study of FKE-2 Building in UTeM

Jahangir Hossain, Hussain Shareef, *Member, IEEE*, Md. Alamgir Hossain, *Senior Member, IEEE*, Akhtar Kalam, *Life Member, IEEE*, and Aida Fazliana Abdul Kadir

***Abstract*—This paper presents a technique for determining the optimal sizing of a hybrid solar photovoltaic (PV) and battery energy storage (BES) system for grid-connected commercial buildings. The objective is to minimize the total net present cost (NPC), which includes the costs of the PV-BES system and electricity expenses. To achieve this, a rule-based energy management system with peak-shaving is implemented using the particle swarm optimization algorithm. The optimization process takes into account actual annual data on solar insolation, air temperature, load consumption, electricity net energy metering (NEM) prices, and the limitation of PV power exporting to the grid. The proposed technique is applied to the configuration of PV-BES systems in Malaysian commercial buildings. The optimization results are validated through uncertainty analysis using ten years of real data. A realistic cash flow analysis is presented, showing the customer's annual payments throughout the project's lifetime. The study focuses on a case study of a grid-connected commercial building (Fakulti Kejuruteraan Elektrik - FKE-2) at Universiti Teknikal Malaysia (UTeM) in Melaka. The results demonstrate reductions of 12.33% in the cost of electricity (COE), 22.62% in annual energy consumption, and 15.85% in peak demand. Furthermore, the proposed optimization technique is implemented and discussed in other states of Malaysia for comparison purposes.**

***Index Terms*—Energy management, commercial buildings, rooftop photovoltaic, battery energy storage management, optimal capacities.**

Manuscript received 18 June 2023; accepted 13 December 2023. Date of publication 15 January 2024; date of current version 21 May 2024. Paper 2023-IACC-0825, presented at the 2023 IEEE IAS Global Conference on Renewable Energy and Hydrogen Technologies (GlobConHT), Male, Maldives, Mar. 11–12, and approved for publication in IEEE TRANSACTIONS ON INDUSTRY APPLICATIONS by the Industrial Automation and Control Committee of the IEEE Industry Applications Society [DOI: 10.1109/GlobConHT56829.2023.10087792]. This work was supported by the Strategic Research Program, UAEU under Grant G00004216 and in part by the Ministry of Higher Education Malaysia under the Fundamental Research Grant Support under Grant FRGS/1/2020/TK0/UTEM/02/66. *(Corresponding authors: Jahangir Hossain; Hussain Shareef.)*

Jahangir Hossain and Aida Fazliana Abdul Kadir are with the Faculty of Electrical Engineering, Universiti Teknikal Malaysia, Melaka, Durian Tunggal 76100, Malaysia (e-mail: hossain614@yahoo; fazliana@utem.edu.my).

Hussain Shareef is with Electrical and Communication Engineering, College of Engineering, United Arab Emirates University, Al Ain 15551, United Arab Emirates (e-mail: shareef@uaeu.ac.ae).

Md. Alamgir Hossain is with Queensland Micro- and Nanotechnology Centre, Griffith University, Nathan, QLD 4111, Australia (e-mail: mdalamgir.hossain@griffith.edu.au).

Akhtar Kalam is with Smart Energy Unit, Victoria University, Melbourne, VIC 3011, Australia (e-mail: akhtar.kalam@vu.edu.au).

Color versions of one or more figures in this article are available at https://doi.org/10.1109/TIA.2024.3353714.

Digital Object Identifier 10.1109/TIA.2024.3353714

NOMENCLATURE

Parameters

P_{fil}^{max}	Maximum feed-in-limit to grid (kW).
P_{d-lim}	Demand limit (kW).
PC_r	Present cost of components replacement (RM).
$N_{pv,b,inv}^{max}$	Maximum number of PV, battery, and inverter.
P_{pv}^{max}	Maximum PV generated power (kW).
P_b^{min}	Battery's minimum power (kW).
P_b^{max}	Battery's maximum power (kW).
SOC^{min}	Battery's minimum SOC (%).
SOC^{min}	Battery's maximum SOC (%).
E_b^{min}	Battery's minimum energy (kWh).
E_b^{max}	Battery's maximum energy (kWh).
E_b	Battery capacity (kWh).
C_s	PV salvage value (RM).
q	Electricity escalate rate (%).
$i,\ d$	Interest rate (%).
Δt	Sampling time.
t	Time.
h	Hour.
L_{pv}	Lifespan of PV (year).
R_{pv}	PV remaining lifetime after project lifespan (year).
N	Lifetime of components (year).
y	Project lifetime (year).
$PC_{O\&M}$	Present cost of operation and maintenance (RM).
$C_{pv,b,inv}$	Component's capital present cost (RM)
C_r	Components replacement cost (RM).
$C_{O\&M}$	Yearly operation and maintenance cost (RM).
CRF_{ele}	Capital recovery factor of electricity.
CRF_{sys}	Capital recovery factor of components.

Variables

P_l	Load demand (kW).
P_g^i, P_e	Import and export power from/to grid (kW).
E_{an}^c	Annual electricity consumption (kWh).
P_{pv}	Output power of PV (kW).
LF	Load factor (%).
$N_{pv,b,inv}$	Number of PVs, batteries, and inverters.
E_c	Annual electricity cost (RM).
P_b	Battery's input and output power (kW).
P_d	Dumped power (kW).
E_{ICPT}^c	Imbalance cost pass-through surcharge (RM).

NPC_{ele}	Electricity net present cost (RM).
NPC_{total}	Configuration's total net present cost (RM).
$TAP_{,grid}$	Total annual payment for grid (RM).
$TAP_{,sys}$	Total annual payment after system implementation (RM).
T_{AP}	Total annual payment of configuration (RM).
$AP_{,\ capex}$	Annual payment for Capex (RM).
$AP_{,opex}$	Annual payment for Opex (RM).
$AP_{,grid}$	Electricity annual payment (RM).
$AB_{,sys}$	Annual benefit of the system configuration (RM).
$T_{B,sys}$	Configuration's total benefit (RM).

I. Introduction

MALAYSIA has been actively promoting the installation of rooftop solar photovoltaic (PV) systems in buildings as a means to generate electricity for the grid. Instead of utilizing outer space for solar energy generation, the focus is on empowering consumers to sell excess electricity back to the grid, accompanied by additional benefits [1]. In line with this, the country announced a four-round tender in May 2020 for the installation of 1 gigawatt (GW) of PV capacity, with the aim of achieving a 20% renewable energy mix in the total power generation by 2025 [2].

The energy consumption of residential and commercial buildings has become a significant contributor, accounting for 40% of the total energy consumption in developing countries. This trend can be attributed to factors such as economic growth, urbanization, population increase, and the growing adoption of electric vehicles [3]. Unfortunately, the energy consumption from buildings also leads to increased greenhouse gas emissions, positioning Malaysia as the 26th largest emitter among 35 countries [3]. Given the finite nature of fossil fuels and the need to mitigate greenhouse gas emissions, it is crucial to explore alternative energy sources.

While the liberalization of the electrical market has resulted in the integration of large-scale renewable energy plants, solar power generation remains the fastest-growing technology among various renewable sources, including hydroelectric, wind, biomass, and tidal energy [4]. However, the intermittent nature of solar energy generation poses a challenge. To address this variability, storage devices can be employed to mitigate fluctuations in PV power supplied to the grid. By storing excess energy during periods of low demand and discharging it during peak hours or at night, energy storage systems can enhance the reliability and stability of solar power utilization. This becomes particularly significant in zero-energy structures, residential dwellings, and under time-of-use (ToU) energy pricing schemes, where power arbitrage entails storing surplus PV energy when prices are low and selling it back to the grid when prices are high.

The economic viability of rooftop PV systems integrated with battery energy storage (BES) for commercial buildings is currently under investigation, primarily due to the higher cost associated with BES [5]. It is essential to carefully select an optimal PV-BES system to ensure the provision of both technical and economic benefits [6]. Achieving these benefits are of utmost importance for grid-connected commercial buildings. Extensive research has been conducted on the optimal planning, sizing, and location of components in power systems [7], residential households with and without BES, and wind turbines [8], [9], standalone PV systems with BES and diesel generators (DG) [10], [11], and microgrids (MG) with and without BES and wind turbines [12], [13]. However, existing literature primarily focuses on determining the optimal capacity for hybrid PV-BES system sizing in grid-connected buildings.

TABLE I
Summary of Existing Works With Limitations

Reference	Realistic parameters ignorance	Components	Load factor (LF) analysis	Cash flow analysis
[14]	Opex	PV-BES	×	×
[15]	Real input data	BES	×	×
[16]-[18]	Grid constraint	PV-BES	×	×
[20], [21]	Flat tariff rates	PV-BES	×	×
[23]	BES limitation	BES	×	×
[24], [25]	BES charging using a grid	PV-BES	×	×
[26], [27]	Salvage value	PV	×	×
[31], [32]	Utility service charge	PV-BES	×	×
This study	-	PV-BES	√	√

A. Literature Review

The optimal sizing of PV-BES systems has been extensively studied in previous articles. However, some crucial practical factors are often overlooked, including grid constraints, actual component costs, real weather conditions, and load data. Neglecting these parameters can result in impractical outcomes. Table I provides a summary of existing works along with their limitations. For instance, in [14], the replacement and maintenance costs of components were neglected when determining the optimal sizing of PV-BES systems. Other studies utilized low-resolution daily electricity load consumption and solar PV generation data for BES sizing [15]. Several investigations failed to consider the maximum and minimum PV export power to the grid as a constraint for optimal sizing in residential and commercial buildings [16], [17], [18]. However, the limitation on exporting PV power to the grid is mainly implemented as a technical constraint based on the power balance guidelines set by the Malaysian Energy Commission [19].

Moreover, most articles focused on residential buildings, microgrids, and islanding, with few providing optimal PV-BES system sizing specifically for commercial buildings without addressing peak demand reduction under flat tariff rates [20], [21]. In the real-world scenario, commercial buildings in Malaysia have electricity consumption prices in RM/kWh and demand charges in RM/kW. The calculation of electricity bills for commercial buildings under the C1 tariff is outlined in [22]. Additionally, in [23], the optimal sizing of PV-BES systems was investigated considering hourly utilization of full battery charging and discharging, accounting for the day-long peak period specified by the C1 tariff (8 a.m. to 10 p.m.). Optimal battery utilization during these peak times becomes crucial to avoid introducing another peak. The primary focus of PV-BES utilization is to reduce peak demand and increase the load factor (LF), which also results in a rebate on energy consumption from the utility company during the off-peak period (10 p.m. to 8 a.m.). However, [24], [25], the utilization of excess PV energy for battery charging is only considered, neglecting the grid as a potential source during an electricity crisis when unavailable PV energy.

Furthermore, in [26], [27], optimal PV sizing for residential buildings was conducted without considering salvage value, which represents the value of the components after the project's lifetime. Incorporating salvage value into the optimal sizing model would yield more precise and realistic results. The contribution of BES systems to the grid for reducing dumped power was not accounted for in [28], [29], [30]. Additionally, in [31], [32], optimal PV-BES system sizing was studied without considering the utility service charge, which is a monthly fee that consumers are required to pay regardless of their actual electricity consumption. Including the utility service charge would lead to more realistic optimization outcomes. Additionally, annual cash flow from commercial bank loans for investment and LF analysis was not examined in earlier studies. Furthermore, there is no restriction considered on the amount of rooftop space for PV that is accessible to clients.

B. Contributions

The objective of this article is to determine the optimal sizing of rooftop solar photovoltaic (PV) and battery energy storage (BES) systems for commercial buildings in Malaysia operating under the C1 tariff. This study builds upon the previous work [5], where a rule-based energy management system (EMS) with peak-shaving and detailed economic analysis was not fully explored. In this article, a rule-based EMS with peak-shaving is developed to ensure the efficient operation of the PV-BES system, taking into account grid constraints and minimizing dumped power. The model incorporates actual annual weather and load data, as well as PV and BES capital investment (Capex), operating expenditure (Opex), appropriate escalation rates, and interest rates. The optimization model for PV and BES is extended to cover all Malaysian states.

The following summarizes the significant contributions of this study compared to earlier publications:

1) Determination of the optimal capacity of PV-BES systems under the C1 tariff in Malaysia using realistic data, enabling the development of a practical optimization technique for grid-connected commercial buildings.
2) Evaluation of annual cash flow analysis for grid-connected PV-BES systems in commercial buildings.
3) Uncertainty analysis of solar insolation and air temperature based on ten years of actual data to assess the robustness of the optimization results.
4) Provision of a practical guideline for selecting the appropriate PV-BES system size based on typical daily electricity consumption and available rooftop space for installation.

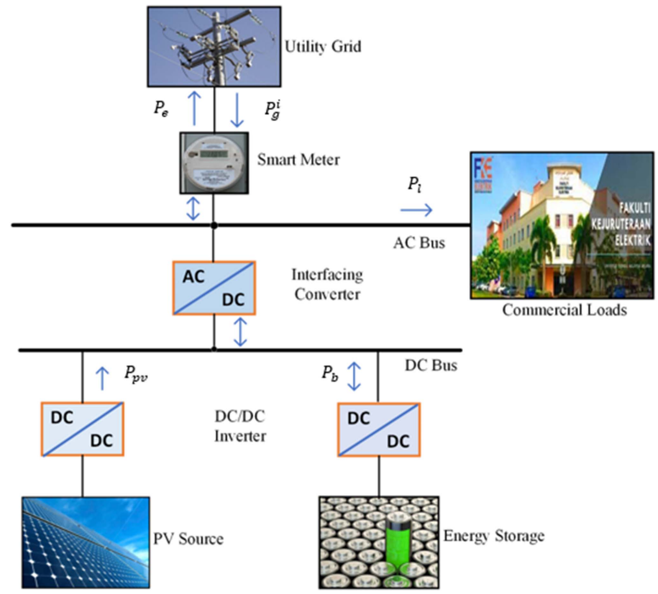

Fig. 1. Proposed system configuration with PV-BES for Malaysian commercial buildings.

5) Instead of solely focusing on reducing PV output fluctuations fed into the grid, the application aims to minimize the net present cost of components while also reducing net power purchases from the grid, considering load, PV, BES, and peak power reduction.

The rest of the article is organized as follows. The system modeling is described in Section II. Section III includes the modeling of an optimization problem. The case study of the FKE-2 building in UTeM is included in Section IV. Results and discussion are presented in Section V. Optimal systems in Malaysian states are implemented in Section VI. The conclusion and future work are drawn in Section VII.

II. System Modeling

A. System Configuration Description

An end-user grid-connected commercial building comprises PV, BES, and grid. The PV and BES are connected to the DC bus through the dc/dc inverter. The interfacing converter or bi-directional converter is connected between the AC and DC buses. The AC commercial loads are connected to the AC bus. The BES is parallel to the PV system. Besides, the grid is the source of both power delivery and absorption. The proposed configuration system is illustrated in Fig. 1.

B. Grid

The grid is a reliable source for largely dependent power demand. Thus, the grid is already connected to the end-user building, this system does not need any construction, operating, and maintenance expenses. The grid is used for satisfying the load demand whenever the load demand falls in a crisis. The usage of supplied electricity from the grid can be expressed as follows.

$$P_g^i(t) = P_l(t) - P_{pv}(t) + P_b(t). \quad (1)$$

C. PV Generator

One of the renewable energy resources is solar energy. PV systems are required to convert directly solar energy into electricity. The generated output power of PV modules likely depends on solar insolation, which can be obtained using (2) [33].

$$P_{pv}(t) = M \times P_{r,pv} \times \frac{G_t}{G_{STC}} \times [1 + C_t(T_c - T_{ref})]. \quad (2)$$

where, P_{pv}, M, and $P_{r,pv}$ are the PV output power, optimal PV sizing units, PV modules' rated power under standard test condition ($T = 25\,^{\circ}$C, $G_{STC} = 1000\,\mathrm{W/m^2}$), and G_t is the solar insolation (W/m^2), respectively. C_t is the temperature coefficient, T_{ref} is 25 °C, T_c is the cell temperature of the PV, which can be calculated by following (3).

$$T_c = T^a + G_t\left(\frac{NOCT - 20}{800}\right). \quad (3)$$

where, T^a is the air temperature, $NOCT$ is the nominal cell operating temperature

C. Battery Energy Storage

PV power generation greatly depends on weather conditions. The BES is utilized to store the surplus power of the PV to support the system voltage and frequency [34] and also deliver the power when less PV power generation or load demand is higher than the demand limit [35]. In this study, excess PV power is stored in the BES for future use. The stored energy of the BES at the time t depends on the previous BES's state-of-charge (SOC), the required loads, and the generated PV power of the system. Therefore, rule-based EMS is designed using mathematical modeling by following charging and discharging rules. The rule-based EMS of proposed configuration is shown in Fig. 2. Since, rule-based EMS is simple, user-friendly, and easy to understand as well. Besides, rules are simply updated based on consumers adoption of real-time pricing (RTP), ToU, and enhanced time-of-use (EToU) tariffs.

1) Discharging Mode 1. Rule 1: When $P_l(t) > P_{d-\mathrm{lim}}$&& $P_{pv}(t) \leq P_l(t) - P_{d-lim}$, the BES is discharged by amount $(P_l(t) - P_{d-lim}) - P_{pv}(t)$.

2) Discharging Mode 2. Rule 2: If PV exported power, $P_e(t)$ <1 kW && $SOC(t) == SOC^{max}$, BES discharge occurs for making up to 1 kW by amount $1 - P_e(t)$.

Rule 3: If $P_e(t) \geq 1$ kW || $P_e(t) < 1$ kW && $SOC(t) < SOC^{max}$, BES is not used for discharging.

3) Charging Mode 1. Rule 4: If $P_l(t) \leq P_{d-lim}$ && $P_{pv}(t) > P_l(t)$ && $P_{pv}(t) - P_l(t) > P_{fil}^{max}$, BES is charged by amount $(P_{pv}(t) - P_l(t)) - P_{fil}^{max}$.

Rule 5: If $P_l(t) \leq P_{d-lim}$ && $P_{pv}(t) > P_l(t)$ && $P_{pv}(t) - P_l(t) < P_{fil}^{max}$, BES is charged by amount $P_{pv}(t) - P_l(t)$.

Rule 6: If $P_l(t) \leq P_{d-lim}$ && $P_{pv}(t) < P_l(t)$, BES is charged by amount $P_{d-lim} - (P_l(t) - P_{pv}(t))$.

4) Charging Mode 2. Rule 7: When $P_l(t) > P_{d-lim}$&& $P_{pv}(t) - (P_l(t) - P_{d-lim}) > P_{fil}^{max}$, BES is charged by amount $P_{pv}(t) - (P_l(t) - P_{d-lim}) - P_{fil}^{max}$.

Rule 8: When $P_l(t) > P_{d-lim}$&&$P_{pv}(t) - (P_l(t) - P_{d-lim}) < P_{fil}^{max}$, BES is charged by amount $P_{Pv}(t) - (P_l(t) - P_{d-lim})$.

where, "||" and "&&" are the logical "OR" and "AND" operators, respectively.

After occuring rule 5 and 8 for BES charging, $P_e(t)$ is determined by (4) and (5).

$$P_e(t) = \min\left(P_{fil}^{max}, (P_{pv}(t) - P_l(t) - P_b(t))\right). \quad (4)$$

$$P_e(t) = \min\left(P_{fil}^{max}, (P_{pv}(t) - (P_l(t) - P_{d-lim}) - P_b(t))\right). \quad (5)$$

Otherwise,

$$P_e(t) = P_{fil}^{max}. \quad (6)$$

The charging and discharging of the BES at each time interval based on the SOC can be determined by (7), and (8), respectively.

$$P_b(t) = \min\left(P_b(t), E_b/h.SOC_{max} - SOC(t-1)\right).\Delta t. \quad (7)$$

$$P_b(t) = -(\min(-P_b(t), E_b/h.(SOC(t-1) - SOC_{min}))).\Delta t. \quad (8)$$

The energy level of the BES is determined by

$$E_b(t) = E_b(t-1) + \eta_{ch} P_b(t).\Delta t - \frac{-P_b(t)}{\eta_d}.\Delta t. \quad (9)$$

The SOC of the BES at each interval is determined as following (10).

$$SOC(t) = (1 - \sigma).\frac{E_b(t)}{E_b^{max}}.\Delta t. \quad (10)$$

where, σ, η_{ch}, and η_d are battery's self-discharging, charging, and discharging efficiency, respectively, which are considered as 1%, 95%, and 98%, respectively.

C. Dumped Power

If the difference between the power generated by the PV system and the load demand exceeds the maximum allowable PV exporting power, the excess power is used to charge the BES. However, if there is still surplus power remaining, it is considered as excess power and is discharged or not utilized further through the control system of the PV system. It can be written by

$$P_d(t) = P_{pv}(t) - P_l(t) - P_{fil}^{max} - P_b(t). \quad (11)$$

In cases where the power generated by the PV system exceeds the load demand by a significant margin, surpassing both the demand limit and the maximum allowable PV exporting power, the surplus PV power is utilized to charge the BES. However, any remaining excess power that cannot be accommodated or utilized further is discharged or not utilized through the PV control system, effectively eliminating the surplus power. It can

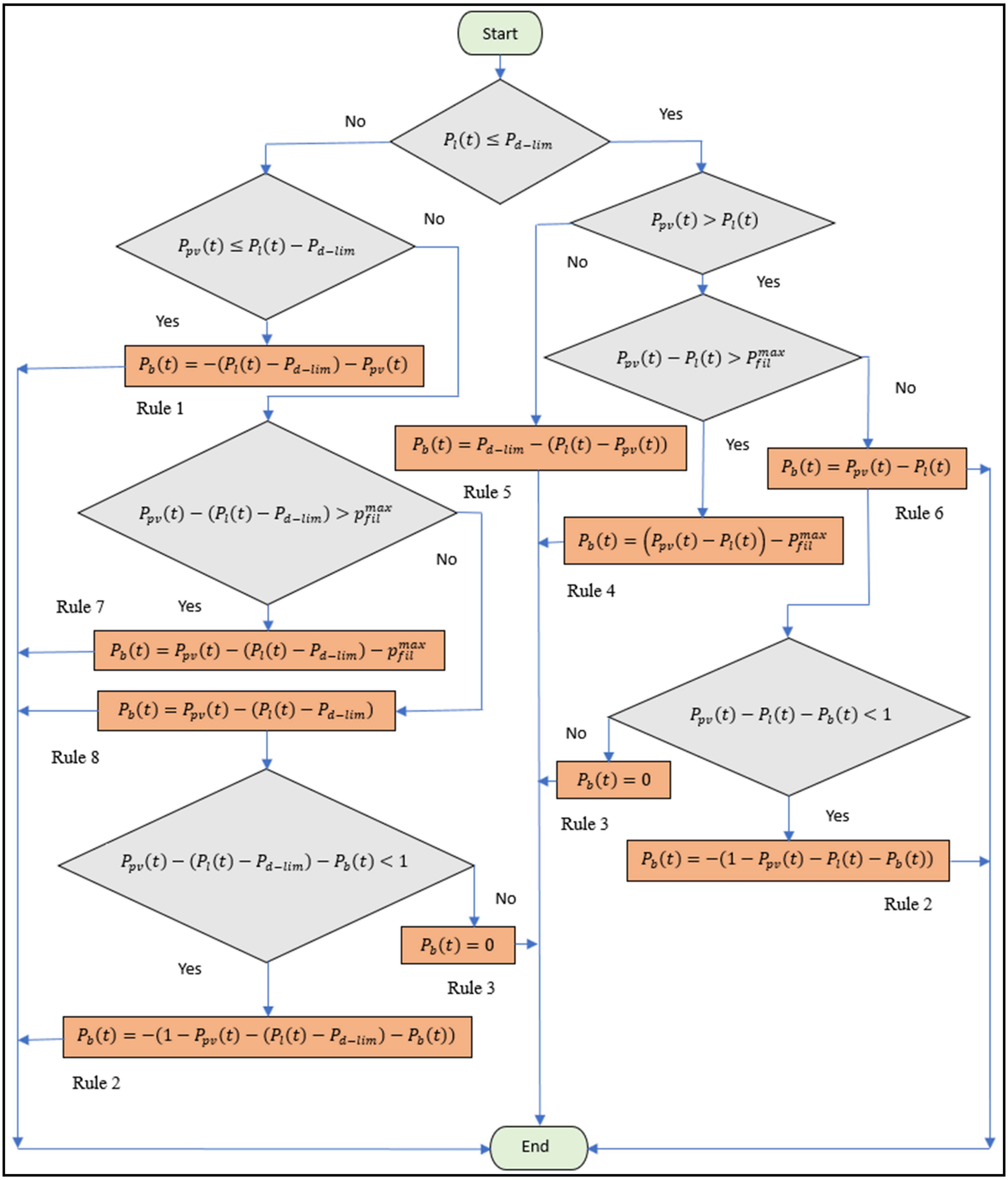

Fig. 2. Rule-based EMS for the proposed configuration of grid-connected commercial buildings in Malaysia.

be obtained by

$$P_d(t) = P_{pv}(t) - (P_l(t) - P_{d-lim}) - P_{fil}^{max} - P_b(t). \quad (12)$$

III. Optimization Modeling

The planning problem in this study is formulated as an optimization model, which can be solved using different optimization solvers in MATLAB. The flowchart of optimization process as shown in Fig. 3. In this case, the particle swarm optimization (PSO) algorithm is employed to solve the optimization problem, as it has demonstrated success in optimal PV-BES sizing for both residential and commercial buildings [36], [37]. PSO offers superiority over other evolutionary algorithms due to its simplicity, low storage requirements, minimal dependency on initial points, and high convergence rate [38]. Compared to other optimization techniques, PSO is less reliant on the initial point set, indicating a higher degree of convergence [39]. The key advantages of PSO over other methods include its simplicity, fewer parameters to be adjusted, its power in solving optimization problems, and its faster performance in power system optimization [40]. In recent years, PSO has been recognized as one of the heuristic optimization strategies for optimizing the sizing of PV-BES systems,

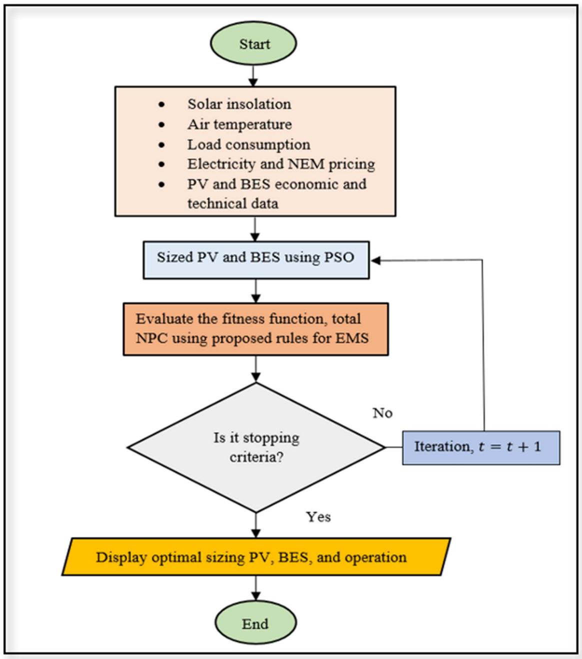

Fig. 3. Optimization process using PSO algorithm through proposed rule-based EMS for determining optimal PV-BES system sizing and operation.

particularly in dealing with challenges related to distributed energy resources (DERs) [41]. Notably, a comparison of three algorithms, including the Imperialistic Competitive Algorithm (ICA), Genetic Algorithm (GA), and PSO, revealed that PSO was the fastest, produced the best solution, and achieved the best results [42]. PSO also outperformed GA and ICA by finding the best solution in fewer iterations. In Section V-F of this article, a comparison between GA and PSO is provided, focusing on factors such as faster convergence rate, number of iterations, and reduction rate of the objective function.

A. Objective Function

The total net present cost (NPC) throughout 20 years lifespan project which is consisted of system NPC (PV-BES) and NPC of electricity that is considered as objective function. Therefore, we have

$$minimize\ f\ NPC_{total} = NPC_{sys} + NPC_{ele}. \quad (13)$$

Equation (14) is used to calculate the NPC_{sys} for PV-BES system, as follows.

$$\begin{aligned} NPC_{sys} = N_{pv}.\left(C_{PV} + PC_{O\&M} - C_s\right) \\ + N_b.\left(C_b + PC_{O\&M} + PC_{r,b}\right) \\ + N_{inv}.\left(C_{inv} + PC_{r,inv}\right). \end{aligned} \quad (14)$$

The present value of fixed annual operation and maintenance cost over a component's lifespan at interest rate i is calculated by

$$PC_{O\&M} = C_{O\&M}.\frac{(1+i)^y - 1}{i(1+i)^y}. \quad (15)$$

The present value of each component repalcement cost after N years of the components lifetime is calculated by

$$PC_r = C_r.\sum_{N=1}^{N<y} \frac{1}{(1+i)^N}. \quad (16)$$

The project lifetime is considered as 20 years period whereas PV lifespan is 25 years. Therefore, the remaining lifetime value of the PV after project lifetime is called the salvage value, which can be calculated by (17).

$$C_s = C_{pv}.\frac{R_{pv}}{L_{pv}}. \quad (17)$$

The imbalance cost pass-through (ICPT) is a surcharge imposed on non-domestic electricity consumers in Malaysia. It is reviewed every consecutive 6 months and is based on factors such as increasing fuel prices, maintenance costs of power plants, and other associated charges [43]. In this study, it is assumed that the ICPT surcharge increases by 1% after each 6-month period. As a result, the annual electricity price is considered to have a 2% increasing rate. The ICPT surcharge is applied to the amount of energy consumed by consumers and is calculated based on the prevailing interest rate, denoted as i. Therefore, the real interest rate can be calculated as follows:

$$d = \frac{i - q}{1 + q} \quad (18)$$

The annual electricity cost for NPC_{ele} is calculated as follows.

$$NPC_{ele} = E_c + E^c_{ICPT}.\frac{(1+d)^y - 1}{d(1+d)^y}. \quad (19)$$

Customers who sign up for the off-peak tariff rider (OPTR) programme will additionally receive a 20% discount on daily energy usage between 10:00 p.m. and 8:00 a.m., but only if their LF for the month is higher than their six-month average LF [43]. To improve LF, the first step is to reduce peak demand at the facility, which will also result in lower monthly electricity expenditures and improved reliability [44].

$$LF = \frac{Total\ energy\ consumption\ monthly\ \ (kWh)}{MD\,(kW) \times 24 \times Days}. \quad (20)$$

The monthly utility service charges are included with annual electricity cost, which 600 RM/ month for C1 tariff in Malaysia. Therefore, we have

$$\begin{aligned} E_c = & \sum_{t=1}^{8760} \sum_{t\in m=1}^{12} \left(P_g^i\,(m) \times 0.365 + MD\,(m) \times 30.30\right) \times \Delta t \\ & - \sum_{t=1}^{8760} NEM\,(t) \times P_e\,(t) \times \Delta t \\ & - \sum_{t=1}^{8760} \sum_{t\in h=22}^{8} \left(P_g^i\,(m) \times 0.365 \times \Delta t\right) \times 0.2 \\ & + \sum_{t=1}^{8760} \sum_{t\in m=1}^{12} U_s^{ch}\,(m) \times \Delta t. \end{aligned} \quad (21)$$

$$E_{ICPT}^{c} = \sum_{t=1}^{8760} \sum_{t \in m}^{12} (P_g^i (m) \times 0.365) \times \Delta t. \quad (22)$$

B. System Constraints

The system design constraints are considered as follows.

$$0 \leq N_{pv,b,inv} \leq N_{pv,b,inv}^{max}. \quad (23)$$

$$0 \leq P_{pv}(t) \leq P_{pv}^{max}. \quad (24)$$

$$P_b^{min} \leq P_b(t) \leq P_b^{max}. \quad (25)$$

$$E_b^{min} \leq E_b(t) \leq E_b^{max}. \quad (26)$$

$$SOC^{min} \leq SOC(t) \leq SOC^{max}. \quad (27)$$

$$P_g^i(t) + P_{pv}(t) + P_b(t) - P_e(t) \geq P_l(t). \quad (28)$$

$$1 \leq P_e(t) \leq P_{fil}^{max}. \quad (29)$$

Equation (23) says the constraint of maximum number of PV, BES, and inverter. The maximum PV power generation is constrained by (24). In (25) and (26) indicate the constraints of BES charging/discharging power and energy, respectively. The SOC of BES is constrained by (27). Equation (28) implies the constraint of power balance at each time interval. The maximum PV exporting power to grid is constrained by (29).

C. Cost of Electricity (COE)

The COE is usually used for comparison between in the presence and absence of PV-BES system. The COE (RM/kWh, RM/kW) is calculated taking into account the NPC of PV-BES system and electricity cost with incorporating cost recovery factor (CRF) of PV-BES system and electricity cost divided by annual electricity consumption.

$$CRF_{sys} = \frac{i(1+i)^y}{(1+i)^y - 1}. \quad (30)$$

$$CRF_{ele} = \frac{d(1+d)^y}{(1+d)^y - 1}. \quad (31)$$

$$E_{an}^c = \sum_{t=1}^{8760} P_l(t) \times \Delta t \,(kWh). \quad (32)$$

$$COE = \frac{NPC_{sys} \times CRF_{sys} + NPC_{ele} \times CRF_{ele}}{E_{an}^c}. \quad (33)$$

IV. UTeM's FKE-2 Building Case Study

The proposed EMS and optimization model for commercial buildings are general techniques that can be implemented in standard networks. This article focuses on investigating the proposed optimization model specifically for a grid-connected commercial building in Malaysia, using the C1 tariff. The case study is conducted at the Fakulti Kejuruteraan Elektrik (FKE-2) commercial building located in the Universiti Teknikal Malaysia (UTeM). The input data for the case study includes two different datasets, one for the technical and economic aspects of the PV-BES system components and grid attributes, and another for the load demand and weather data. These datasets are utilized to analyze the technical and economic feasibility of implementing the PV-BES system in the commercial building.

TABLE II
PV-BES System Cost, Electricity, and NEM With Interest and Escalate Rates

PV	Capital cost = RM 1458/kW Operation & maintenance cost = RM 75/kW	PV lifespan = 25 years Solar panel efficiency = 20%
BES	Capital cost = RM 1850/kWh Operation & maintenance cost = RM 30/kWh Replacement cost = RM 1055/kWh	BES lifespan = 10 years SOC^{min} = 20% SOC^{max} = 100%
Inverter	Capital cost = RM 2440/kW Replacement cost = RM 1508/kW	Inverter lifetime = 10 years
Electricity Cost	Retail price = 0.365 RM/kWh, and 30.30 RM/kW, NEM = 0.365 RM/kWh	Interest rate, i = 8% Escalate rate, q = 2%

A. Technical and Economic Data

The parameters, component costs, grid electricity and NEM pricing, as well as the electricity escalation and interest rates, are provided in Table II [45]. All the costs and pricing are in Malaysian ringgit (RM), based on the actual market prices in Malaysia. The objective function of the optimization model aims to minimize the total NPC over a 20-year project lifespan. The degradation of the BES system, which occurs due to cyclic and calendar aging, is indirectly incorporated by considering a round-trip efficiency of 80% over the project period. In 2019, Malaysia implemented a maximum NEM power limitation, which states that after self-consumption of PV power by the load, the surplus PV power should not exceed 75% of the consumer's maximum demand and should not be less than 1 kW at the connection point [19]. This grid constraint is imposed to ensure the safe operation of the grid and prevent overloading issues.

B. Load Demand Profile and Weather Data

The annual load consumption for the FKE-2 building at UTeM in Malaysia is illustrated in Fig. 4(a). Over the course of a year, the maximum and average electricity consumption values are 82.39 kW and 17.59 kW, respectively. Furthermore, the average daily energy consumption is 422.047 kWh, while the annual energy consumption amounts to 154057 kWh. It is worth noting that Malaysia experiences an average solar radiation ranging from 400 to 600 MJ/m^2 per month [46]. Fig. 4(b) displays the daily solar insolation and air temperature data recorded in Melaka, Malaysia, throughout the year 2021.

V. Results and Discussion

The proposed optimization approach is applied to the FKE-2 commercial building in UTeM, which falls under the C1 tariff for

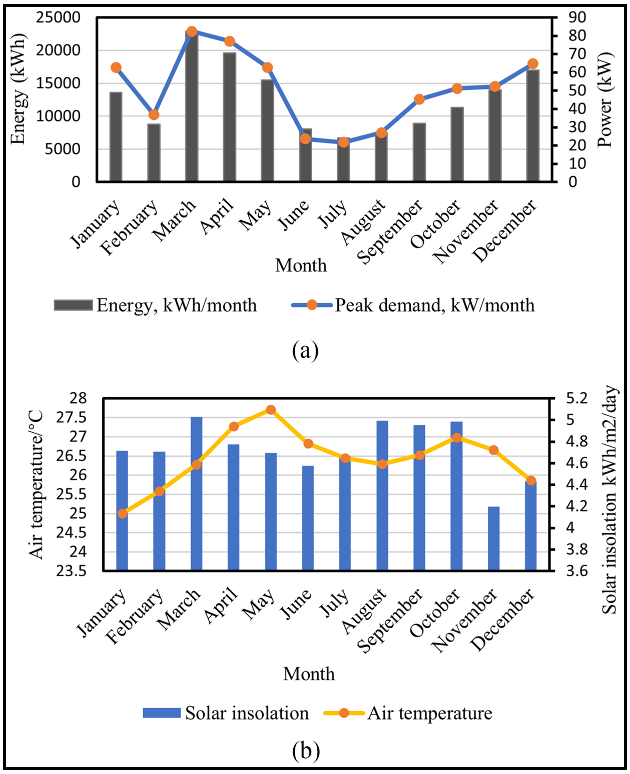

Fig. 4. (a) Load consumption of FKE-2 commercial building in UTeM. (b) Solar insolation, and air temperature of Melaka, in Malaysia.

TABLE III
OPTIMIZATION RESULTS FOR PROPOSED CONFIGURATION

PV (kW)	BES (kWh)	Total NPC (RM)	COE (RM/kWh)	AGEI (kWh)	AEEG (kWh)	ADE (kWh)	APDD (%)	AECD (%)
25	22.4	521,487	0.32	119,000	6250.62	50.68	15.85	22.62

commercial buildings. Various simulation results are obtained to evaluate and discuss the configuration. The study presents the results of sensitivity analysis for daily optimal operation, cash flows, and uncertainty analysis, along with a comparison discussion on the convergence of PSO and GA. The sensitivity analysis aims to provide guidance to customers in selecting the optimal PV-BES system for their commercial buildings in Malaysia.

A. Optimal Rooftop PV and BES Capacities

The results for the proposed configuration are presented in Table III, including the optimal PV-BES system capacity, total NPC, COE, AGEI (annual grid energy import), AEEG (annual export energy to the grid), ADE (annual dumped energy), APDD (annual peak demand reduction), and AECD (annual energy consumption reduction). The optimal configuration determined for this case is a combination of 25 kW of PV capacity and 22.4 kWh of BES capacity. The COE achieved is 0.32 RM/kWh, which corresponds to a 12.33% reduction compared to a system without PV-BES. The surplus PV energy is exported to the grid after meeting the load demand and charging the BES. A total

TABLE IV
MONTHLY LF FOR A YEAR WITH 20% DISCOUNT

Previous 6 months/average LF	Present month/LF	20% rebate during (10 p.m. to 8 a.m.)
Jul-Dec/0.3111	Jan/0.4726	Applicable
Aug-Jan/0.3144	Feb/0.3732	Applicable
Sept-Feb/0.3142	Mar/0.4799	Applicable
Oct-Mar/0.3228	Apr/0.4418	Applicable
Nov-Apr/0.3388	May/0.4403	Applicable
Dec-May/0.3399	Jun/0.5891	Applicable
Jan-Jun/0.3635	Jul/0.4136	Applicable
Feb-Jul/0.3838	Aug/0.4231	Applicable
Mar-Aug/0.3872	Sept/0.3672	NA
Apr-Sept/0.3704	Oct/0.2986	NA
May-Oct/0.3629	Nov/0.3922	Applicable
Jun-Nov/0.4284	Dec/0.3927	NA

of 6250.62 kWh of energy is sold to the grid using the 25 kW PV capacity. The AGEI is reduced by 22.62%, corresponding to 119000 kWh, thanks to the PV-BES system. The ADE is 50.68 kWh, indicating the contribution of the BES in reducing dumped energy. Furthermore, the optimal system configuration results in a 15.85% reduction in peak demand and a 22.27% reduction in the average monthly electricity bill for the C1 tariff. It is worth noting that the optimal PV-BES system supplies 26.82% of the commercial building's demand.

B. Load Factor Analysis

The electrical LF is a measure of the efficiency or utilization rate of electrical energy usage. A higher LF indicates more efficient utilization of electrical energy. Improving the LF is primarily focused on controlling peak demand. By reducing peak demand, the LF percentage automatically improves. A low load factor suggests that consumers are using electricity inefficiently compared to what they could achieve with better peak demand control. The load factor is particularly useful for evaluating the benefits of BES strategies and demand control.

For the FKE-2 commercial building in UTeM, the average load factor over the past six months was recorded as 0.3111. Based on this load factor, the monthly load factors for the entire year are compared to the load factor of the previous six months for those who have signed up for OPTR to receive a 20% discount on energy consumption between 10:00 p.m. and 8:00 a.m. Table IV presents the 20% discount over the twelve months of the year. The 20% discount applies to all months except September, October, and December.

C. Cash Flow Analysis for Annual Payment

During the project's lifetime, the cash flow analysis implies the customers' annual payment for each year. The capital/replacement/maintenance cost of PV, BES, and inverter are loaned from commercial bank with at low interest rate in Melaka, Malaysia. The total annual payment for the FKE-2 commercial building is as follows.

$$TAP_{,sys} = AP_{,capex} + AP_{,opex} + AP_{,grid}. \quad (34)$$

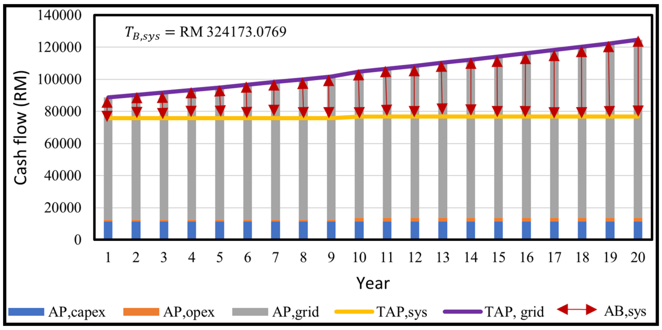

Fig. 5. Cash flow analysis over a project lifetime with $AB_{,sys}$ and $T_{B,sys}$.

The 20-year annual cash flow analysis for the proposed system is depicted in Fig. 5. After 10 years, the annual payment increases due to the replacement costs of the inverter and BES in the proposed system configuration. The annual revenue generated from selling excess power back to the grid is lower than the total annual payment for imported electricity. The difference between two lines (purple and gold) represents the annual benefit, $AB_{,sys}$ for each year with the proposed system configuration's total benefit, $T_{B,sys}$ and the total annual payment, $TAP_{,sys}$.

Over the 20-year lifetime, the average $AB_{,sys}$ is more than RM 16208 per year. Additionally, the average difference in total annual payment, $TAP_{,sys}$ throughout the 20-year period is RM 13188 for the optimal PV-BES system. This indicates that consumers can save an average of up to RM 13188 per year with the proposed configuration in terms of annual payment. Moreover, the total benefit, $T_{B,sys}$ amounts to RM 324173.0769 when using the optimal PV-BES system. This value is more representative of the realistic electricity costs for commercial buildings under the C1 tariff, which includes charges in RM/kWh (unit energy cost) and RM/kW (demand cost).

D. Daily Optimal Operation Analysis

As Malaysia is located in the equator region, the weather remains relatively consistent throughout the year. It is important to investigate and evaluate the optimal system operation and power flow of the proposed configuration. Figs. 6 and 7 illustrates the daily operation strategies for two specific days, showcasing how the system operates on a daily basis.

1) Case 1: Lower Load Demand With Higher PV Generation Availability: If $P_l(t) < P_{d-lim}$, battery is charged using grid when PV power generation is not available during $t = 2$, 3, 4, 5, 6, 7, 21, 22, 23, and 24 h. When PV power generation is available and $P_l(t) < P_{d-lim}$, PV power is fed to the load, then battery is used for charging purpose. It can be observed at $t = 8$, 9, 10, 11, 12, 18, 19, and 20 h. If $P_l(t) > P_{d-lim}$, and $P_{pv}(t) > (P_l(t) - P_{d-lim})$, the amount $P_{pv}(t) - (P_l(t) - P_{d-lim})$ of excess PV power is sold to the grid at time $t = 16$ h, after battery charging based on SOC, which is during $t = 15$, and 17 h. Since, during $t = 17$ h, excess PV power was less than 1 kW, which was made up by battery discharging to 1 kW to sell to the grid, whereas the battery was fully charged at the maximum SOC level as shown in Fig. 6(c). The optimal battery charging and discharging schedule is shown in Fig. 6(b). For this case, there is no dumped power, which is shown in Fig. 6(a). The import power from the grid after utilization of PV and batteries is shown in Fig. 6(d).

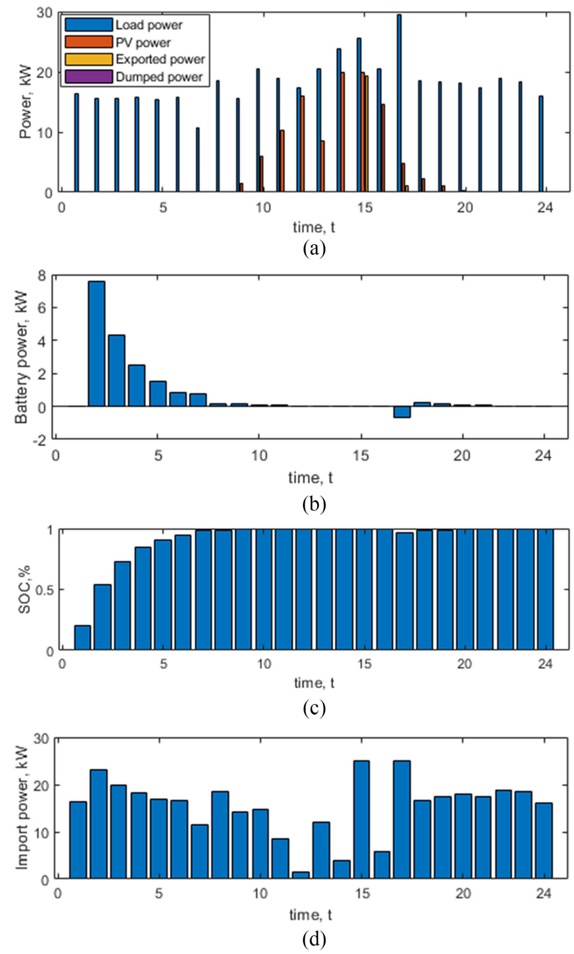

Fig. 6. Analysis of daily power flow for proposed configuration in two sample days. Case 1. (a) Load demand, PV power, export power, and dumped power. (b) Battery charging/discharging scheduling. (c) SOC of the battery. (d) Grid import power.

2) Case 2: Higher Load Demand With Lower PV Generation Availability: If $P_l(t) < P_{d-lim}$, grid is utilized for battery charging when PV power generation is not available during $t = 1$, 2, 3, 4, 5, 6, 7, 20, 21, 22, 23, and 24 h. When $P_l(t) < P_{d-lim}$, PV power is available, then it is fed to the load and charging the battery during $t = 8$, 18, and 19 h. If $P_l(t) > P_{d-lim}$, and $P_{pv}(t) < (P_l(t) - P_{d-lim})$, the amount $(P_l(t) - P_{d-lim}) - P_{pv}(t)$ is discharged battery based on SOC, when $t = 9$, 10,11,14, and 16 h. If $P_l(t) > P_{d-lim}$, and $P_{pv}(t) > (P_l(t) - P_{d-lim})$, and $P_{pv}(t) > (P_l(t) - P_{d-lim})$, the amount $P_{pv}(t) - (P_l(t) - P_{d-lim})$ of excess PV power is sold to the grid at time $t = 12$, 13, and 15 h. When $t = 17$ h, excess PV is firstly used for battery charging, and the remaining is dumped as less than 1 kW as shown in Fig. 7(a), and the battery's SOC is not equal to its maximum SOC. Since, the battery's charging and discharging cannot occur at the same time, the battery's optimal schedules for charging and discharging are shown in Fig. 7(b).

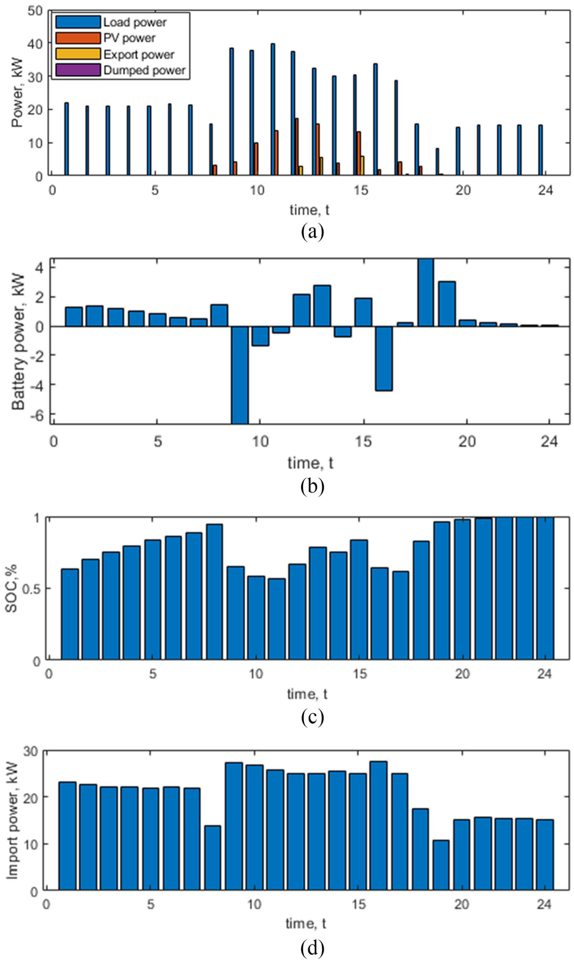

Fig. 7. Analysis of daily power flow for proposed configuration in two sample days. Case 2. (a) Load demand, PV power, export power, and dumped power. (b) Battery charging/discharging scheduling. (c) SOC of the battery. (d) Grid import power.

The SOC of the battery and the import of power from the grid are illustrated in Fig. 7(c) and (d), respectively.

E. Uncertainty Analysis Using Last 10 Years Data

To validate the findings of the proposed methodology, an uncertainty analysis is conducted considering the variability in solar insolation and air temperature. Real data collected from the Melaka urban area in Malaysia over a 10-year period (2011-2020) is used for this analysis. Fig. 8(a) displays the annual average air temperature and the daily average solar insolation during this period. Fig. 8(b) presents the optimal capacities of the PV-BES system for the proposed configuration over the 10-year period. It is observed that the optimal PV capacity ranges from 28 kW for three years, 30 kW for two years, and 25 kW for five years. Similarly, the optimal BES capacity varies, with 14 kWh for two years, 18 kWh for two years, 20 kWh for one year, and 22.4 kWh for five years.

This uncertainty analysis confirms that the optimal PV-BES capacities obtained in Section V-A are suitable for typical commercial buildings in Malaysia, considering an average daily consumption of 422.047 kWh and a maximum allowable PV export power limit of 25 kW to the grid.

F. PSO and GA Convergence Comparison for Proposed Optimization Model

The proposed optimization problem for determining the optimal PV-BES system is solved using the PSO algorithm. The objective is to minimize the total NPC, which consists of both PV-BES system costs and electricity costs. PSO is chosen as a robust optimization method to find the optimal configuration that minimizes the objective function. The capacity of the PV and BES components are considered as control variables in the optimization process. The formulated problem's objective function is a nonlinear fitness function, and it is solved using the PSO and GA solvers in MATLAB. Both PSO and GA are popular heuristic methods commonly used for solving nonlinear optimization problems [47]. In this study, the population size for the optimization process is set to 30. Comparing the performance of PSO and GA, it is observed that the PSO algorithm requires fewer iterations and less computation time to reach the optimal solution, as shown in Fig. 9(a) and (b), respectively.

VI. Optimal Systems in Malaysia States

The proposed optimization approach, along with the system configuration shown in Fig. 1, is also applied to different states in Malaysia. Real data specific to each state is used, including solar insolation, air temperature, electricity pricing, and the NEM scheme. The average values of solar insolation, air temperature, electricity pricing, and NEM scheme for Malaysian states are provided in Table V. Malaysia is divided into two regions: Peninsular Malaysia (West Malaysia) and East Malaysia (Borneo States). Peninsular Malaysia consists of 11 states, while East Malaysia comprises 3 states that are geographically separated from the mainland. It is important to note that electricity prices vary between Peninsular Malaysia and East Malaysia. The NEM scheme is applicable to all states in Peninsular Malaysia, except for Sabah in East Malaysia. Additionally, the Sunday tariff rider, which exempts the electricity peak demand charge on Sundays, is only applicable to Sabah and not to other states in Malaysia. The electricity demand charge and off-peak tariff rider are not applicable in Sarawak. Among all the states in Malaysia, Sabah exhibits the highest daily average solar insolation of 5.21 kWh/m^2 and an average daily air temperature of 27.9 °C. This indicates that installing PV systems in Sabah can potentially yield greater benefits compared to other states. However, it's important to note that the NEM scheme is not applicable in Sabah, requiring careful consideration in selecting the optimal PV-BES system for this region. Fig. 10 presents a comparison of the optimal PV-BES sizing with the COE for various states in Malaysia.

It observed that Selangor and Johor show the minimum impact on COE when utilizing solar PV due to their lower solar insolation. On the other hand, the lowest COE is found in Sarawak, Kelantan, Penang, and Perak, indicating that these states experience a significant reduction in COE with the implementation of PV-BES systems. Melaka, Kedah, and Perlis also demonstrate a reasonable COE reduction (from RM 0.365 to RM 0.32) since these three states have similar daily average solar insolation.

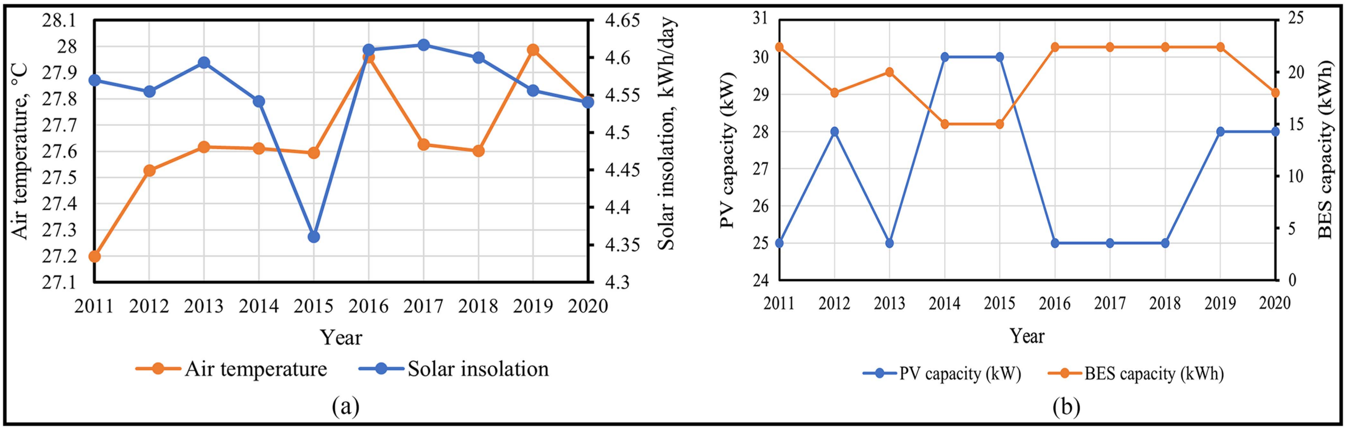

Fig. 8. Uncertainty analysis with 10 years real data (2011-2020). (a) Solar irradiance and air temperature. (b) Optimal PV and BES capacity for each year.

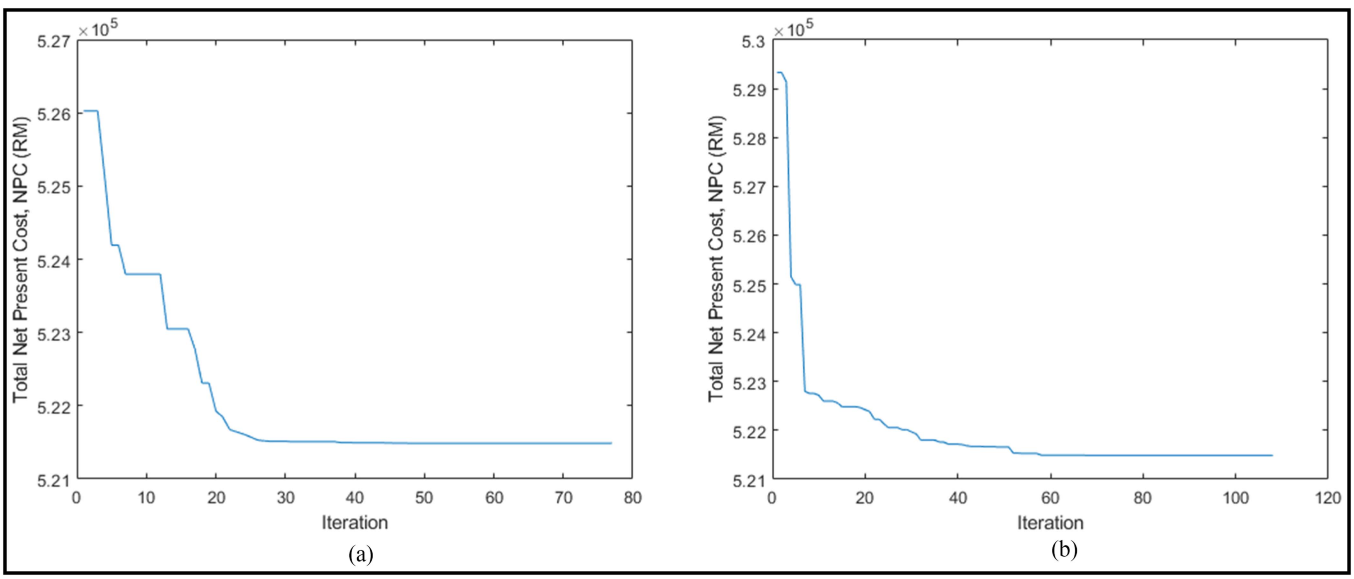

Fig. 9. (a) Characteristics convergence of proposed PSO algorithm. (b) Characteristics convergence of GA algorithm.

TABLE V
ELECTRICITY AND NEM PRICING WITH METEOROLOGICAL REAL DATA FOR ALL STATES OF MALAYSIA

	States of Malaysia	**daily average temperature (ºC)**	**Solar insolation of daily average (kWh/m2)**	**Electricity price (RM/kWh) C1 tariff**	**Electricity price (RM/kW) C1 tariff**	**NEM rates (RM/kWh)**	**Off Peak tariff rider**	**Sun day tariff rider for C1 tariff**	**Monthly utility service charge (RM)**
Peninsular Malaysia	Johor	25.9	4.45	0.365	30.30	0.365	Applicable	N/A	600
	Kedah	28.45	4.83	0.365	30.30	0.365	Applicable	N/A	600
	Kelantan	27.5	4.96	0.365	30.30	0.365	Applicable	N/A	600
	Melaka	26.7	4.83	0.365	30.30	0.365	Applicable	N/A	600
	Negeri Sembilan	25.7	4.64	0.365	30.30	0.365	Applicable	N/A	600
	Pahang	24.1	4.67	0.365	30.30	0.365	Applicable	N/A	600
	Penang	26.6	4.96	0.365	30.30	0.365	Applicable	N/A	600
	Perak	25.8	4.91	0.365	30.30	0.365	Applicable	N/A	600
	Perlis	26.7	4.84	0.365	30.30	0.365	Applicable	N/A	600
	Terengganu	26.1	4.72	0.365	30.30	0.365	Applicable	N/A	600
	Selangor	26.1	4.31	0.365	30.30	0.365	Applicable	N/A	600
East Malaysia	Sarawak	27.4	5.09	0.32	N/A	0.32	N/A	N/A	10
	Sabah	27.9	5.21	0.324	23.20	N/A	Applicable	Applicable	1000

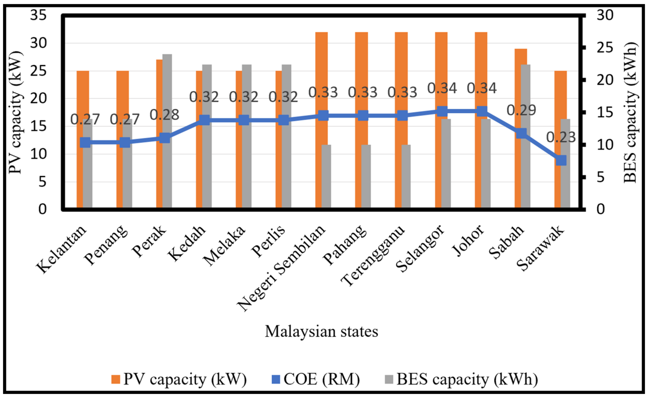

Fig. 10. COE comparison of proposed configuration for different Malaysian states.

Overall, Malaysia benefits from abundant solar insolation, which serves as a strong motivation for installing PV systems with BES. However, it is important to note that according to the sustainable energy development authority (SEDA), the generated PV energy should first be consumed through load feeding, and any surplus can be sold. Therefore, the remaining PV generation can be efficiently used to charge the battery, allowing for optimal utilization of the BES and effectively reducing the peak demand.

In summary, the comparison of optimal PV-BES sizing with COE highlights the potential for COE reduction in various states of Malaysia. While states with lower solar insolation may experience a smaller effect on COE, overall, the country's ample solar insolation provides a favorable environment for PV system installations, which can be further enhanced through the integration of BES technology.

VII. Conclusion and Future Work

This study focused on optimizing PV-BES systems for grid-connected commercial buildings in Melaka, Malaysia. By utilizing real annual data on solar insolation, air temperature, and load consumption, the study successfully determined the optimal capacity for the PV and BES components. The results showed that a 25 kW PV system combined with a 22.4 kWh BES could achieve a 12.33% reduction in the COE for a typical commercial building in Melaka.

Furthermore, the optimized PV-BES system demonstrated significant benefits in terms of energy consumption and peak demand reduction, with respective reductions of 22.62% and 15.85%. Over the lifespan of the project, the total benefit ($T_{B,sys}$) for the PV-BES system was estimated to be RM 324173.0769. Uncertainty analysis using real data from the previous ten years confirmed the stability of the optimal PV-BES system capacity over this period, providing valuable guidance for the proper sizing of PV-BES systems in commercial buildings.

Additionally, the study extended its investigation to different states in Malaysia. It was found that Sarawak offered the most profitable opportunities for PV-BES systems, thanks to lower utility service charges and demand charges, coupled with the second-highest daily average solar insolation among the states. Melaka also showed potential for PV-BES system installations, emphasizing the importance of battery utilization for peak demand reduction. Given that peak demand charges account for a significant portion (30–70%) of electricity costs for commercial buildings in Malaysia, the proper sizing and implementation of PV-BES systems can lead to substantial cost savings.

The optimal planning of the PV-BES system can be further enhanced by integrating an electrolyser to utilize surplus PV energy and reduce peak demand. This approach eliminates wasted power and provides additional benefits from the electrolyser, which uses the excess energy that would have otherwise been dumped. The optimization model remains the same, but the electricity cost calculation in (21) would include the added benefit of the electrolyser, which has the potential to significantly reduce peak demand. However, the implementation of a rule-based EMS is necessary to maximize the peak demand reduction for commercial buildings in Malaysia. Furthermore, a comprehensive guideline can be developed to assist consumers in leveraging government subsidies, incentives, and upcoming electricity programs introduced by the Malaysian government specifically tailored for commercial buildings in the future.

References

[1] Malaysian Sustainable Energy Development Authority (SEDA), 2022. [Online]. Available: https://www3.seda.gov.my/iframe/

[2] Malaysian Sustainable Energy Development Authority (SEDA), 2022. [Online]. Available: https://www.seda.gov.my/reportal/wp-content/uploads/2021/12/MyRER_webVer-1.pdf

[3] J. Hossain et al., "A review on optimal energy management in commercial buildings," *Energies*, vol. 16, no. 4, Feb. 2023, Art. no. 1609, doi: 10.3390/en16041609.

[4] T. Kërçi, G. Tzounas, and F. Milano, "A dynamic behavioral model of the long-term development of solar photovoltaic generation driven by feed-in tariffs," *Energy*, vol. 256, Oct. 2022, Art. no. 124506, doi: 10.1016/j.energy.2022.124506.

[5] J. Hossain, A. F. A. Kadir, H. Shareef, and M. A. Hossain, "Hybrid PV and battery system sizing for commercial buildings in Malaysia: A case study of FKE-2 building in UTeM," in *Proc. IEEE IAS Glob. Conf. Renewable Energy Hydrogen Technol.*, 2023, pp. 1–6, doi: 10.1109/GlobConHT56829.2023.10087792.

[6] C. Mokhtara, B. Negrou, N. Settou, B. Settou, and M. M. Samy, "Design optimization of off-grid hybrid renewable energy systems considering the effects of building energy performance and climate change: Case study of Algeria," *Energy*, vol. 219, Mar. 2021, Art. no. 119605, doi: 10.1016/j.energy.2020.119605.

[7] H. M. Al-Masri and M. Ehsani, "Feasibility investigation of a hybrid on-grid wind photovoltaic retrofitting system," *IEEE Trans. Ind. Appl.*, vol. 52, no. 3, pp. 1979–1988, May/Jun. 2016, doi: 10.1109/TIA.2015.2513385.

[8] R. Khezri, A. Mahmoudi, and M. H. Haque, "A demand side management approach for optimal sizing of standalone renewable-battery systems," *IEEE Trans. Sustain. Energy*, vol. 12, no. 4, pp. 2184–2194, Oct. 2021, doi: 10.1109/TSTE.2021.3084245.

[9] A. A. R. Mohamed, R. J. Best, X. Liu, and D. John Morrow, "A comprehensive robust techno-economic analysis and sizing tool for the small-scale PV and BESS," *IEEE Trans. Energy Convers.*, vol. 37, no. 1, pp. 560–572, Mar. 2022, doi: 10.1109/TEC.2021.3107103.

[10] R. Ayop, N. M. Isa, and C. W. Tan, "Components sizing of photovoltaic stand-alone system based on loss of power supply probability," *Renewable Sustain. Energy Rev.*, vol. 81, pp. 2731–2743, Jan. 2018, doi: 10.1016/j.rser.2017.06.079.

[11] T. Khatib, A. Mohamed, K. Sopian, and M. Mahmoud, "Optimal sizing of building integrated hybrid PV/diesel generator system for zero load rejection for Malaysia," *Energy Buildings*, vol. 43, no. 12, pp. 3430–3435, Dec. 2011, doi: 10.1016/j.enbuild.2011.09.008.

[12] S. B. Sepúlveda-Mora and S. Hegedus, "Resilience analysis of renewable microgrids for commercial buildings with different usage patterns and weather conditions," *Renewable Energy*, vol. 192, pp. 731–744, Jun. 2022, doi: 10.1016/j.renene.2022.04.090.

[13] S. Bandyopadhyay, G. R. C. Mouli, Z. Qin, L. R. Elizondo, and P. Bauer, "Techno-economical model based optimal sizing of PV-battery systems for microgrids," *IEEE Trans. Sustain. Energy*, vol. 11, no. 3, pp. 1657–1668, Jul. 2020, doi: 10.1109/TSTE.2019.2936129.

[14] B. Zou et al., "Capacity configuration of distributed photovoltaic and battery system for office buildings considering uncertainties," *Appl. Energy*, vol. 319, Aug. 2022, Art. no. 119243, doi: 10.1016/j.apenergy.2022.119243.

[15] Y. Ru, J. Kleissl, and S. Martinez, "Storage size determination for grid-connected photovoltaic systems," *IEEE Trans. Sustain. Energy*, vol. 4, no. 1, pp. 68–81, Jan. 2013, doi: 10.1109/TSTE.2012.2199339.

[16] B. Zou, J. Peng, S. Li, Y. Li, J. Yan, and H. Yang, "Comparative study of the dynamic programming-based and rule-based operation strategies for grid-connected PV-battery systems of office buildings," *Appl. Energy*, vol. 305, Jan. 2022, Art. no. 117875, doi: 10.1016/j.apenergy.2021.117875.

[17] G. Subramani et al., "Techno-economic optimization of grid-connected photovoltaic (PV) and battery systems based on maximum demand reduction (MDRED) modelling in Malaysia," *Energies*, vol. 12, no. 18, Sep. 2019, Art. no. 3531, doi: 10.3390/en12183531.

[18] A. A. F. Husain, M. H. A. Phesal, M. Z. A. Ab Kadir, and U. A. Ungku Amirulddin, "Techno-economic analysis of commercial size grid-connected rooftop solar pv systems in Malaysia under the nem 3.0 scheme," *Appl. Sci. (Switzerland)*, vol. 11, no. 21, Nov. 2021, Art. no. 10118, doi: 10.3390/app112110118.

[19] Malaysia Energy Commission, 2019. Accessed: Feb. 2023. [Online]. Available: Guidelines for solar photovoltaic installation on net energy metering scheme_energy_commision_Malaysia_registrationrecord.pdf

[20] N. S. Kelepouris, A. I. Nousdilis, A. S. Bouhouras, and G. C. Christoforidis, "Cost-effective hybrid PV-battery systems in buildings under demand side management application," *IEEE Trans. Ind. Appl.*, vol. 58, no. 5, pp. 6519–6528, Sep./Oct. 2022, doi: 10.1109/TIA.2022.3186295.

[21] N. Iqtiyani Ilham, N. Yenita Dahlan, M. Zhafran Hussin, and S. Alam, "Assessing techno-economic value of battery energy storage with grid-connected solar PV compensation schemes for malaysian commercial prosumers," *Int. J. Renewable Energy Res.*, vol. 12, pp. 759–767, 2022.

[22] Malaysian utility company, Tenaga Nasional Berhad (TNB), Nov. 2022. [Online]. Available: https://www.tnb.com.my/commercial-industrail/pricing-tariff1/

[23] J. Li, "Optimal sizing of grid-connected photovoltaic battery systems for residential houses in Australia," *Renewable Energy*, vol. 136, pp. 1245–1254, Jun. 2019, doi: 10.1016/j.renene.2018.09.099.

[24] R. Khezri, A. Mahmoudi, and M. H. Haque, "Optimal capacity of solar PV and battery storage for Australian grid-connected households," *IEEE Trans. Ind. Appl.*, vol. 56, no. 5, pp. 5319–5329, Sep./Oct. 2020, doi: 10.1109/TIA.2020.2998668.

[25] Y. Zhang, A. Lundblad, P. E. Campana, F. Benavente, and J. Yan, "Battery sizing and rule-based operation of grid-connected photovoltaic-battery system: A case study in Sweden," *Energy Convers. Manage.*, vol. 133, pp. 249–263, 2017, doi: 10.1016/j.enconman.2016.11.060.

[26] M. Mehrtash, F. Capitanescu, P. K. Heiselberg, T. Gibon, and A. Bertrand, "An enhanced optimal PV and battery sizing model for zero energy buildings considering environmental impacts," *IEEE Trans. Ind. Appl.*, vol. 56, no. 6, pp. 6846–6856, Nov./Dec. 2020, doi: 10.1109/TIA.2020.3022742.

[27] S. Bandyopadhyay, G. R. C. Mouli, Z. Qin, L. R. Elizondo, and P. Bauer, "Techno-economical model based optimal sizing of PV-battery systems for microgrids," *IEEE Trans. Sustain. Energy*, vol. 11, no. 3, pp. 1657–1668, Jul. 2020, doi: 10.1109/TSTE.2019.2936129.

[28] A. M. Abdelshafy, H. Hassan, and J. Jurasz, "Optimal design of a grid-connected desalination plant powered by renewable energy resources using a hybrid PSO–GWO approach," *Energy Convers. Manage.*, vol. 173, pp. 331–347, Oct. 2018, doi: 10.1016/j.enconman.2018.07.083.

[29] S. B. Sepúlveda-Mora and S. Hegedus, "Resilience analysis of renewable microgrids for commercial buildings with different usage patterns and weather conditions," *Renewable Energy*, vol. 192, pp. 731–744, Jun. 2022, doi: 10.1016/j.renene.2022.04.090.

[30] R. Khezri, A. Mahmoudi, and M. H. Haque, "Optimal capacity of PV and BES for grid-connected households in South Australia," in *Proc. IEEE Energy Convers. Congr. Expo.*, 2019, pp. 3483–3490.

[31] M. Alramlawi and P. Li, "Design optimization of a residential PV-battery microgrid with a detailed battery lifetime estimation model," *IEEE Trans. Ind. Appl.*, vol. 56, no. 2, pp. 2020–2030, Mar./Apr. 2020, doi: 10.1109/TIA.2020.2965894.

[32] R. Atia and N. Yamada, "Sizing and analysis of renewable energy and battery systems in residential microgrids," *IEEE Trans. Smart Grid*, vol. 7, no. 3, pp. 1204–1213, May 2016, doi: 10.1109/TSG.2016.2519541.

[33] S. B. Jeyaprabha and J. V. Milanovic, "Probabilistic techno-economic design of isolated microgrid," *IEEE Trans. Power Syst.*, vol. 38, no. 6, pp. 5267–5277, Nov. 2023, doi: 10.1109/TPWRS.2022.3216386.

[34] V. Vijayan, A. Mohapatra, S. N. Singh, and C. L. Dewangan, "An efficient modular optimization scheme for unbalanced active distribution networks with uncertain EV and PV penetrations," *IEEE Trans. Smart Grid*, vol. 14, no. 5, pp. 3876–3888, Sep. 2023, doi: 10.1109/TSG.2023.3234551.

[35] R. Manojkumar, C. Kumar, S. Ganguly, and J. P. S. Catalao, "Optimal peak shaving control using dynamic demand and feed-in limits for grid-connected PV sources with batteries," *IEEE Syst. J.*, vol. 15, no. 4, pp. 5560–5570, Dec. 2021, doi: 10.1109/JSYST.2020.3045020.

[36] J. Khoury, R. Mbayed, G. Salloum, and E. Monmasson, "Optimal sizing of a residential PV-battery backup for an intermittent primary energy source under realistic constraints," *Energy Buildings*, vol. 105, pp. 206–216, Aug. 2015, doi: 10.1016/j.enbuild.2015.07.045.

[37] H. Awad, K. M. E. Salim, and M. Gül, "Multi-objective design of grid-tied solar photovoltaics for commercial flat rooftops using particle swarm optimization algorithm," *J. Building Eng.*, vol. 28, Mar. 2020, Art. no. 101080, doi: 10.1016/j.jobe.2019.101080.

[38] M. A. Hossain, R. K. Chakrabortty, M. J. Ryan, and H. R. Pota, "Energy management of community energy storage in grid-connected microgrid under uncertain real-time prices," *Sustain. Cities Soc.*, vol. 66, Mar. 2021, Art. no. 102658, doi: 10.1016/j.scs.2020.102658.

[39] N. Ghorbani, A. Kasaeian, A. Toopshekan, L. Bahrami, and A. Maghami, "Optimizing a hybrid wind-PV-battery system using GA-PSO and MOPSO for reducing cost and increasing reliability," *Energy*, vol. 154, pp. 581–591, Jul. 2018, doi: 10.1016/j.energy.2017.12.057.

[40] M. A. Hossain, H. R. Pota, S. Squartini, F. Zaman, and J. M. Guerrero, "Energy scheduling of community microgrid with battery cost using particle swarm optimisation," *Appl. Energy*, vol. 254, Nov. 2019, Art. no. 113723, doi: 10.1016/j.apenergy.2019.113723.

[41] M. R. Bonyadi and Z. Michalewicz, "Analysis of stability, local convergence, and transformation sensitivity of a variant of the particle swarm optimization algorithm," *IEEE Trans. Evol. Computation*, vol. 20, no. 3, pp. 370–385, Jun. 2016, doi: 10.1109/TEVC.2015.2460753.

[42] H. HassanzadehFard and A. Jalilian, "Optimal sizing and siting of renewable energy resources in distribution systems considering time varying electrical/heating/cooling loads using PSO algorithm," *Int. J. Green Energy*, vol. 15, no. 2, pp. 113–128, 2018.

[43] Malaysian utility company, Tenaga Nasional Berhad (TNB). 2022. [Online]. Available: https://www.tnb.com.my/commercial-industrial/discounts-rebates-offers/

[44] A. Amir, H. Shareef, and F. Awwad, "Load factor improvement in a standalone microgrid using battery energy storage system," in *Proc. 3rd Int. Conf. Smart Grid Renewable Energy, Proc., Inst. Elect. Electron. Engineers Inc.*, 2022, pp. 1–5, doi: 10.1109/SGRE53517.2022.9774233.

[45] T. Chowdhury, H. Chowdhury, K. S. Islam, A. Sharifi, R. Corkish, and S. M. Sait, "Resilience analysis of a PV/battery system of health care centres in Rohingya refugee camp," *Energy*, vol. 263, Jan. 2023, Art. no. 125634, doi: 10.1016/j.energy.2022.125634.

[46] J. Hossain, N. A. Algeelani, A. H. Hamood Al-Masoodi, and A. F. A. Kadir, "Solar-wind power generation system for street lighting using Internet of Things," *Indonesian J. Elect. Eng. Comput. Sci.*, vol. 26, no. 2, pp. 639–647, May 2022, doi: 10.11591/ijeecs.v26.i2.pp639-647.

[47] W. K. A. Najy, H. H. Zeineldin, and W. L. Woon, "Optimal protection coordination for microgrids with grid-connected and islanded capability," *IEEE Trans. Ind. Electron.*, vol. 60, no. 4, pp. 1668–1677, Apr. 2013, doi: 10.1109/TIE.2012.2192893.

[48] Malaysia Sustainable Energy Development Authority (SEDA). 2022, [Online]. Available: https://Feed-intariff(FiT)inMalaysia.pdf